Mordenite Acidity: Dependence on the Si/Al Ratio and the Framework Aluminum Topology. 2. Acidity Investigations

Helmut Stach,* Jochen Jänchen, Hans-Georg Jerschkewitz, Ursula Lohse, Barbara Parlitz,

Central Institute of Physical Chemistry, O-1199 Berlin, Germany

and Michael Hunger

Department of Physics, University of Leipzig, Leipzig, Germany *(Received: March 16, 1992; In Final Form: June 19, 1992)*

The acidity of a series of mordenites dealuminated by acid refluxing was studied by calorimetric measurements of the NH_3 chemisorption, proton magic angle spinning nuclear magnetic resonance spectroscopy, and temperature-programmed desorption of NH_3 and NH_4^+ ion exchange. The number of bridged OH groups determined by ^1H MAS NMR corresponds to the number of tetrahedrally coordinated Al atoms. Starting with a low Al content (a high Si/Al ratio), the number of the strong acidic sites increases with increasing Al number of the framework up to 4.6 Al atoms/u.c. (Si/Al ratio of 9.5) and then decreases. The decrease of the strong acidity above 4.6 Al atoms/u.c. may be explained by the appearance of an aluminum atom in the second coordination sphere of the Si–OH–Al group. The experimentally found value of the maximum (at $m = 0.096$) in the curve of the strong acidity versus the aluminum molar fraction coincides with a value calculated by Barthomeuf from the topological Al density of mordenite, thus confirming her theoretical concept of zeolite acidity.

Introduction

Correlations between the catalytic activity and the acid strength of H-mordensites are often found. Investigations of the acidity were not always performed precisely, because only a few methods allow determination of the acid strength of microporous catalysts exactly. We investigated dealuminated H-mordenites (with Si/Al_f ratios between 7 and 48) using several methods to characterize their physicochemical properties (see part 1). In this part, results of the investigations of the H-mordenite acidity are presented using four different methods to determine the number of acid sites. Adsorption calorimetry was employed to measure the acid strength and acid strength distribution of the H-mordenites studied accurately.

Experimental Section

Ammonium Exchange Capacity Measurements. The ammonium exchange was performed three times at 343 K as a batch process with an excess of 0.2 N NH_4NO_3 solution (pH = 5.6). The amount of the exchanged NH_4 ions was obtained from the NH_3 content using the Kjeldahl method. The results are given in Table V (column 2) of part 1.

Temperature-Programmed Desorption (TPD) of Ammonia. Prior to the measurements the samples were activated at 773 K in a helium stream for 1 h. After adsorption of ammonia from a helium stream (3 vol %) at 393 K the samples were washed with helium and heated under a stream of helium with a heating rate of 12 K/min. The desorbed amount of NH_3 was measured by a thermal conductivity detector as well as by titration with 0.1 N H_2SO_4. The TPD curves are depicted in Figures 7 and 8 and the calculated amounts of desorbed ammonia are given in Table V of part 1.

Calorimetric Measurements. For the measurement of the differential molar heat of chemisorption of ammonia a microcalorimeter of Calvet-type was used. It was connected with a volumetric sorption apparatus thus enabling the measurement of the evolving heat and the adsorbed amount at the same time. All samples were evacuated ($p < 1$ mPa) at elevated temperatures (653 K) for about 15 h prior to the calorimetric experiments.

All measurements were made at 423 K. Earlier our systematic studies[1] of temperature dependence of the ammonia adsorption showed, in accordance with literature data,[2] that at lower temperatures not all strong acidic sites were obtained and at a much higher temperature decomposition of the formed NH_4^+ ions could occur. Adsorption equilibrium was attained within 4–24 h depending on the amount adsorbed. It was controlled by the heat transition (thermokinetic curve) as well as the mass transition (pressure recording by a capacity membrane manometer of Baratron type). The mean error of the heat of adsorption amounted to approximately 2%. The calorimetric curves are presented in Figure 3.

Results

Temperature-Programmed NH_3 Desorption. Figures 1 and 2 present some results on the temperature-programmed desorption of ammonia. In accordance with data in the literature,[3-5] in the TPD spectra two separate peaks were found. While the maximum temperature of the first peak (low-temperature peak) is practically independent of the degree of dealumination, the maximum temperature of the second (high-temperature peak) decreases with decreasing Al content of the framework (see Table V or part 1). A decrease of the peak maximum temperatures in the TPD spectra can be correlated with a decrease in the acid strength.[6] Therefore, it may be concluded that with a greater degree of dealumination the acid strength of the dealuminated mordenites diminishes.

By investigating dealuminated zeolites of the HZSM-5 type, we found that the spectra of the NH_3 TPD also consist of two peaks.[7] A comparison of the total number of strong acid sites (measured calorimetrically) with the TPD results showed that only the population of the high-temperature peaks corresponded to the calorimetric data. Thus it could be concluded that the low-temperature peak is due not to strong but to weak acid sites. This seems justifiable in the case of the mordenites, too. As will be shown later, the number of strong acid sites derived from the high-temperature peak and from calorimetric measurements of ammonia adsorption are indeed in good agreement.

As is seen in Figure 2, the high-temperature peaks are not symmetric and possess some shoulders especially for zeolites with a high Al content in the framework. Therefore, it appears that ammonia was released from more than two different types of sites with different activation energy of desorption, i.e., different acid strengths.

Similar results were found by Karge et al.[4] after investigating dealuminated mordenites by TPD of ammonia and pyridine. Using a Gaussian distribution function for the probability density of the activation energy of desorption and under special assumptions, a deconvolution of the spectra was possible. Best results were obtained assuming four different types of sites (two Lewis and two Brønsted sites) differing in number and acid strength.

* Corresponding author. Present address: Adlershofer Umweltschutztechnik und Forschungsgesellschaft mbH, Rudower Chaussee 5, 0-1199 Berlin, Germany.

0022-3654/92/2096-8480$03.00/0 © 1992 American Chemical Society

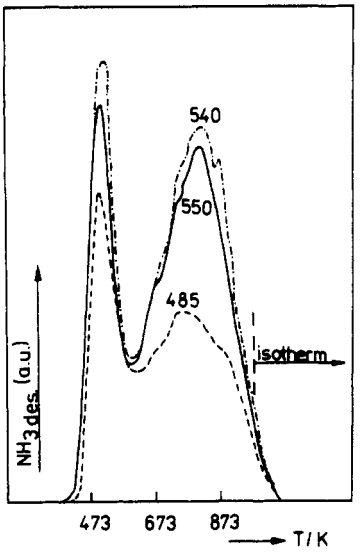


Figure 1. Ammonia TPD spectra of HM-O, HM-Ob and HM-Oc (---, HM-O, — HM-Ob; -·-, HM-Oc).

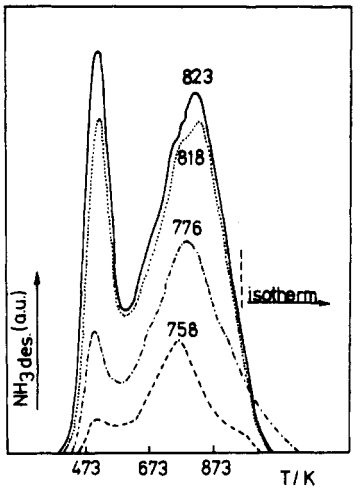


Figure 2. Ammonia TPD spectra of selected dealuminated mordenites (—, HM-Ob, ···, HM-2, -·-, HM-4b, ---, HM-6).

Though the experimental TPD curves are well fitted by the mathematical procedure mentioned, it seems possible that the calculated most frequent activation energies for the ammonia desorption not only reflect the acid strength but may also be influenced by diffusion (as it is the case in nearly all experiments which use dynamic methods).

More precise information on the acidity (especially about the acid strength) should be obtainable by direct exact measurement of the interaction energy of the acid sites with basic molecules, for example, with ammonia.

Calorimetric Measurements. In Figure 3, the differential molar heats of ammonia chemisorption are plotted as a function of the adsorbed number of the basic molecules. In preliminary experiments[1] and in accordance with the literature,[2,8] it was found that a temperature of 423 K was sufficient to obtain reproducible data. Therefore, all measurements were performed at that temperature. It follows from Figure 3 that most of the curves of the dealuminated mordenites show a continuous decrease of the differential molar heats of ammonia adsorption with increasing adsorbed amount. This indicates the existence of a rather broad distribution of adsorption sites with different interaction energy, i.e., different acid strength. The same conclusion was derived (vide supra) from the TPD investigation.

Of special interest is the curve of the heat of ammonia adsorption on Na-mordenite (Figure 3). In this sample all acid sites are neutralized by the Na^+ ions with the consequence that the calorimetrically measured interaction energies are smaller if

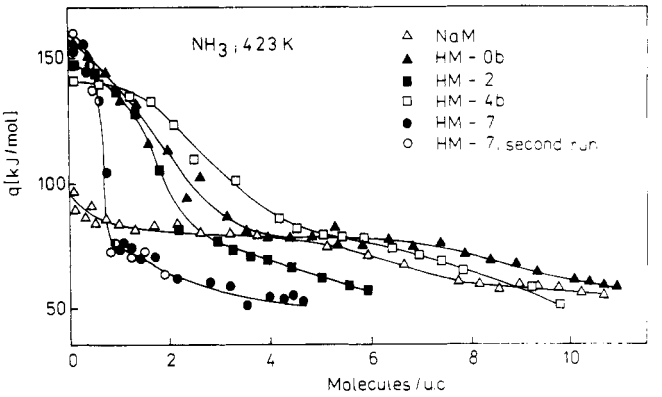


Figure 3. Calorimetric differential molar heats of ammonia adsorption at 423 K (△, NaM; ▲, HM-Ob; ■, HM-2; □, HM-4b; ●, ○, HM-7).

compared with the H form of the mordenites. The curve is characterized by a broad step at about 80 kJ/mol in accordance with data given in ref 9. Comparing the curves depicted in Figure 3 with those found in calorimetric measurements of ammonia adsorption on synthesized mordenites (with nearly the same Si/Al ratio) a very similar behavior can be seen.[2] We conclude that an adsorption heat of about 80 kJ/mol corresponds to the interaction of the ammonia molecules with the oxygen atoms of the framework (and in the case of NaM as well with the sodium cations), i.e., to the physical adsorption. Diminishing the number of aluminum atoms in the framework results in a decreasing field strength and hence in a reduced heat of physical adsorption as is indeed seen in Figure 3.

Heats of adsorption >80 kJ/mol are due to the interaction of ammonia with acid sites.[8-10] The heat of adsorption is proportional to the acid strength: the greater the heat, the higher the acid strength. The number of the chemisorbed ammonia molecules is determined by the intercept of the heat curve with the 80 kJ/mol mark. As is seen in Figure 3 the strength of the acid sites depends on the Si/Al ratio. The initial heat of chemisorption amounts to about 160 kJ/mol for the sample HM-Ob, decreases with rising Si/Al ratio to about 140 kJ/mol, and then increases again. Calorimetric data in the literature for the initial heats of adsorption in the same system are still higher and reach values of about 160–170 kJ/mol.[2,8,10-12] These differences may be due to different experimental conditions or differences in the investigated mordenites.

A comparison of the initial heat of chemisorption of ammonia on dealuminated H-mordenites with those found by us for HY zeolites[13] reveals a substantial difference. The interaction energy of ammonia and therefore the acid strength of the mordenites at low coverages are higher than the corresponding data of the HY molecular sieves. This agrees with the well-known behavior of both zeolites in catalytic reactions[14-18] and the conclusions drawn from the investigations of the acidity by different methods.[19] If the results of the acid strength of dealuminated mordenites here given are compared with our measurements of the acidity of dealuminated HZSM-5 zeolites,[20] it can be found the differences will be small. Concerning the overall initial acid strengths the H forms of the dealuminated zeolites investigated may be arranged in the following rank: HM > HZSM-5 > HY.

Discussion

Influence of the Si/Al_f Ratio on the Total Number of Acid Sites. In Figure 4 the total number of the acid sites (derived by TPD, NH_4 exchange, or calorimetric measurements) of the dealuminated mordenites are plotted against the tetrahedral aluminum content of the unit cell. Additionally, calorimetric data of Tsutsumi et al.[2] are included. Our results show a linear relationship coinciding with the diagonal. The authors attribute the systematic deviations of the results given in ref 2 from the diagonal to a partial conversion of Brønsted into Lewis sites, or an extraction of aluminum atoms from the framework. From the strong linearity of our results in the figure, it can be concluded that every acid site corresponds to a framework aluminum atom and that all acid sites

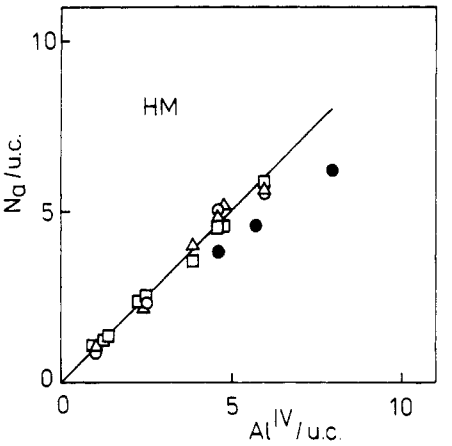


Figure 4. Total number of acid site (per unit cell) dependence on the Al^{IV} content/u.c. of H-mordenites from different methods of measurement (○, calorimetry; ●, calorimetry data from ref 2; △, TPD; □, NH_4^+-exchange capacity).

TABLE I: Comparison of the Total Number of Brønsted Acid Sites Obtained from Different Experimental Methods

sample	N_a^a (mmol/g)	N_a^b (mmol/g)	N_a^c (mmol/g)	N_a^d (mmol/g)	$N_{a,av}/Al_f^e$
HM-Ob	2.04	1.93	1.94	1.78	0.94
HM-1	1.61	1.80		1.57	1.02
HM-2	1.56	1.67	1.73	1.42	1.03
HM-3	1.26	1.40		1.16	0.97
HM-4a	0.83			1.02	1.04
HM-4b	0.86	0.81	0.79	0.90	1.04
HM-4c	0.49			0.62	1.00
HM-4d	0.39			0.50	1.00
HM-6	0.38	0.39	0.29		1.00
HM-7	0.33			0.36	0.90

[a] Ammonium ion exchange capacity. [b] Temperature programmed desorption of ammonia. [c] Calorimetric measurement of ammonia chemisorption. [d] ^1H Magic angle spinning nuclear magnetic resonance. [e] Average value from N_a^a, N_a^b, N_a^c.

are of Brønsted type. The same conclusion was drawn from our measurements of the acidity of dealuminated Y zeolites using four independent methods.[13] Applying the ^1H and ^{27}Al MAS NMR technique, Pfeifer and co-workers[21] also proved the proportionality between the decrease of framework aluminum and the number of bridged hydroxyl groups acting as Brønsted sites in Y zeolites.

But besides the data presented in ref 2, there are several further investigations on dealuminated and synthesized mordenites with different Si/Al ratio, showing that the N_a/Al_f ratio is not close to 1.0 (as in our results, see Table I) but smaller. This follows from Figure 5 on comparing the results of ammonia TPD and of calorimetric measurements of the adsorption heat of ammonia by several authors,[2,3,9] with our data.

As follows from Figure 5, the total numbers of acid sites we measured are larger (for the same number of Al atoms per unit cell) than those found by the authors mentioned. This is not surprising in the case of TPD measurements,[3] because the authors reported only the number of acid sites corresponding to the high-temperature peak. The smaller total number of acid sites derived from calorimetric measurements in refs 2 and 9 may be due to difficulties in the correct determination of the Si/Al ratio and the preparation of the H forms of aluminum-rich mordenites.

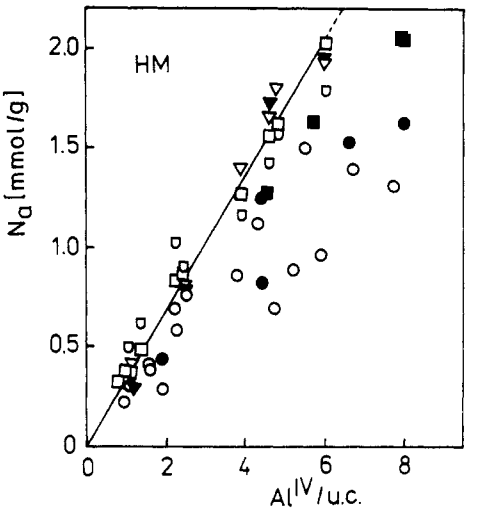


Figure 5. Comparison of the total number of acid sites (mmol/g) as a function of the Al^{IV} content/u.c. of H-mordenites from different measurements (own data: ▼, calorimetry; ▽, TPD, □, ^1H MAS NMR; ●, calorimetry, ref 9; ■, calorimetry, ref 2; ○, TPD, ref 3).

While Sawa et al.[3] reported that above an Al atom content of 5.6 per u.c. the total number of acid sites decreases with increasing amount of Al atoms as did Klyachko et al.,[9] Tsutsumi et al.[2] did not find such an effect. We did not investigate H-mordenites with more than 6 Al atoms per unit cell. But one has to bear in mind that the samples (reported in ref 3) with an Al content above 5.6 (which is equal to a Si/Al ratio above 7.8) do not belong to the same dealumination series but are of different origin.

Influence of the Si/Al_f Ratio on the Acid Strength. From theoretical investigations on zeolites with different Al content per unit cell, an increase of the acid strength with rising Si/Al ratio can be predicted.[23,24] Mortier,[25] using the principles of electronegativity equilization, calculated the average partial charge of the protons in the H forms of several zeolites (faujasites) and found that the charge changed from 0.12 (Si/Al = 1) to 0.14 (Si/Al = 2.5) and 0.18 (Si/Al = infinity). The increase of the ionic character of the H atoms was explained by the relative increase of the Si content of the framework, having a higher electronegativity (compared with Al), and thus shifting the electron density from the proton to the oxygen atom. Therefore, the OH bond in the Si-richer zeolites becomes more ionic and the acid strength rises.

Quantum chemical calculations also allow the conclusion that with rising Si/Al ratio the average T–O–T bond angles increase as well. The consequence is a decrease of the deprotonation energy of the hydroxyl group which results in a higher acidity of the dealuminated zeolites.[26,27]

Following the models of Mortier and Sauer, we have to conclude that the acid strength rises with increasing Si/Al ratios, i.e., with decreasing Al content of the framework in the dealuminated mordenites. The higher acid strength of the samples with a lower Al_f content should be reflected by a higher heat of ammonia chemisorption and by a larger number of the acid sites with a high chemisorption heat. As follows from Figure 3, we find qualitatively such a behavior. To compare the above-mentioned conclusions with the results of our calorimetric measurements more quantitatively, we defined three groups of sites with different acid strengths (with $q > 80$ kJ/mol, $q > 100$ kJ/mol and $q > 120$

TABLE II: Distribution of the Acid Strength of Dealuminated Mordenites

sample	Si/Al_f	m	N_a^a (mmol/g)	N_a^b (mmol/g)	N_a^c (mmol/g)	N_a^d (mmol/g)	N_a^e (mmol/g)
HM-Ob	7.0	0.125	1.94	1.13	0.81	0.23	0.58
HM-2	9.5	0.096	1.73	0.54	1.19	0.33	0.86
HM-4b	18.0	0.052	0.79	0.11	0.68	0.15	0.53
HM-7	47.9	0.021	0.29	0.03	0.26	0.02	0.24

[a] Total number of acid sites with $q > 80$ kJ/mol. [b] Number of acid sites with $80 < q < 100$ kJ/mol. [c] Number of acid sites with $q > 100$ kJ/mol. [d] Number of acid sites with $100 < q < 120$ kJ/mol. [e] Number of acid sites with $q > 120$ kJ/mol.

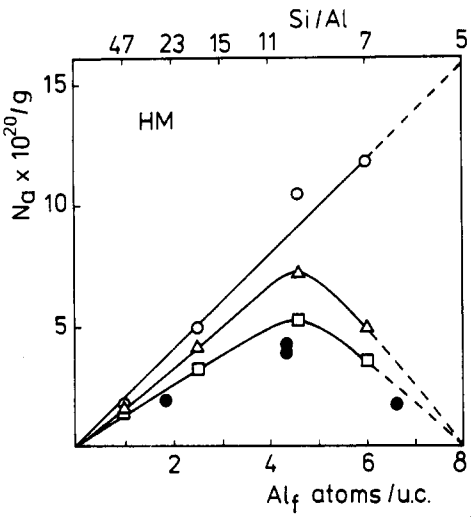


Figure 6. Acid strength distribution dependence on Al^{IV} content per unit cell of dealuminated H-mordenites (○, N_a with $Q > 80$ kJ/mol; △, N_a with $Q > 100$ kJ/mol; □, N_a with $Q > 120$ kJ/mol; ●, data from ref 9).

kJ/mol; see Table II) and determined the corresponding number of acid sites for every group. Whereas the theoretical investigations considered an ideal crystal structure, our measurements concerned the real structure of the mordenite samples with the consequence that we discovered an overlapping of the sites with different acid strength resulting in a broad distribution of the acid strength.

In Figure 6 the acid strength distribution dependence of the dealuminated mordenites on the Si/Al ratio is depicted. (Included also are results given in ref 8. These data agree well with our finding.) As follows from Figure 6, the number of strong acid sites indeed rises with increasing Si/Al ratio. But this correspondence is valid only up to a Si/Al ratio of about 9. Above this value the number of strong acid sites diminishes. An analogous dependence of the strong acid sites on the Si/Al ratio was also found in our calorimetric investigations of dealuminated HY zeolites.[13] It seems to be necessary that the theoretical studies consider the local environment of the hydroxyl groups in the framework more precisely, especially the arrangement of the Al atom having a dominant influence on the acidity.

Following the model of Barthomeuf,[28] the curves of the strong acid sites in Figure 6 may be explained as follows: At a high Si/Al ratio and a consequently low aluminum content, in the unit cell nearly all Al atoms are isolated, possessing a high acid strength (expressed by a heat of chemisorption with $q > 120$ kJ/mol). With increasing number of Al in the lattice, the number of the strong acid sites rises. If there are Al atoms instead of Si atoms in the second coordination sphere, the number of strong acid sites diminishes, although the total number of acid sites increases further. The effect of next-nearest Al atoms on the acidity was interpreted earlier by (i) an influence of close neighbors as in solution or (ii) an overall effect comparable to collective properties in solution.[29] From quantum chemical studies it follows that due to the closeness of the Al atoms, the Si–OH–Al angles change, with the consequence that the acidity decreases.[30]

Topological Density and Acid Strength. Several models were developed to explain the influence of the Al atom in the second coordination sphere on the acidity.[31-34] The main ideas are (i) that strong acidity is connected with isolated Al atoms and (ii) that strong acidity reaches a maximum value at that Si/Al ratio of the lattice at which no next Al neighbor exists in the second coordination sphere. It should be of special interest to consider the structure and topology of the zeolites since the arrangement and distribution of the neighbors of a given Si–OH–Al group determines the acidity of the zeolites, as was pointed out by Barthomeuf.[28]

From a practical point of view as well as from theoretical interest, it is therefore important to determine the limiting Si/Al ratio below which aluminum atoms should have no aluminum as next nearest neighbors (NNN). ^{29}Si MAS NMR spectroscopy

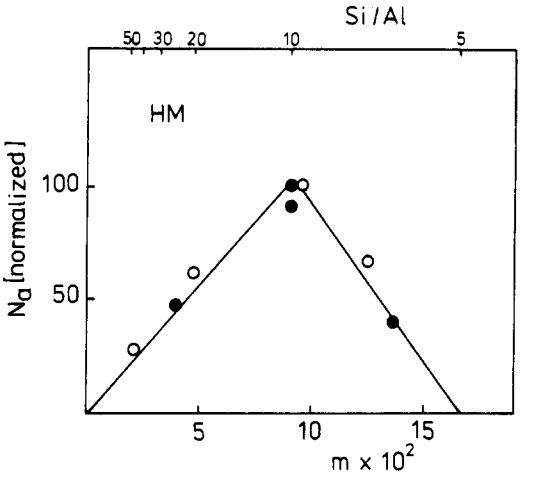


Figure 7. Dependence of the number of strong acid sites on the mole fraction of tetrahedrally coordinated Al atoms (○, own calorimetric data; ●, data from ref 9).

seems to be the only experimental method to give information on the Al distribution in the T sites of a zeolite. But its application becomes difficult in the case of dealuminated materials, as has been shown (cf. part 1 of this paper).

Barthomeuf showed[28] that the topology of zeolites gives information on the way in which the tetrahedra are interconnected and thus how to determine the limiting Si/Al ratios. She started with the topological density of the T atoms (TD_{2-5}). These values can easily be calculated from the coordination sequences.[35] (In mordenite the number of T atoms around an AlO_4 tetrahedron in the second layer amounts to 12, in faujasites only to 9.) Its value is taken over the second to the fifth coordination layer of tetrahedra around a T site divided by the maximum number of T atoms. The TD_{2-5} values are independent of chemical composition, structure symmetry and unit cell.[28] Multiplying the TD_{2-5} value by the molar fraction of aluminum (m), an aluminum topological density may be derived (TD_{Al}). A limiting value of TD_{Al} (limit TD_{Al}) can be calculated for zeolites below which none of the AlO_4 tetrahedra will have another AlO_4 as next-nearest neighbor. Under the assumption that in any zeolite structure the limiting aluminum topological density is the same and using an experimentally determined value of the limit $TD_{Al} = 2.65 \times 10^{-2}$ (for faujasites), it is possible to calculate the limiting values of the aluminum molar fraction (limit m_{NNN}) for other zeolite structures. This procedure allows one to calculate in advance the limiting Si/Al ratio below which Al atoms should have no aluminum as next-nearest neighbors.

Barthomeuf calculated a limiting m_{NNN} value of 0.096 for mordenites. This number corresponds excellently with our experimental finding as follows from Figure 7.

In Figure 7 the number of very strong acid sites ($q > 120$ kJ/mol) is plotted against the aluminum molar fraction of the dealuminated mordenites. Included are also results given by Klyachko et al.[9] Their calorimetric measurements of ammonia chemisorption were performed on synthetic and dealuminated mordenites. The agreement between both sets of calorimetric measurements is very good. (It could be argued that only one measured point may not be enough to prove the decrease in curvature of strong acid sites, but as follows from Figure 7 the independently measured value in the critical range of composition is strong evidence, as well as the complete curve given by Klyachko et al.[9] for the decrease of the number of strong acid sites with diminishing Si/Al ratio.)

Moreover, Barthomeuf predicted a linear increase of the effective strong acidity on mordenite from $m = 0$ to limiting m_{NNN} and then a decrease to zero for the idealized composition of the unit cell. As follows from Figure 7 our results completely fulfill this prediction, thus proving the validity of the theoretical model of Barthomeuf.[28]

Acid Strength and Catalytic Activity. Hydrogen mordenites are frequently studied catalysts in the reactions of paraffin

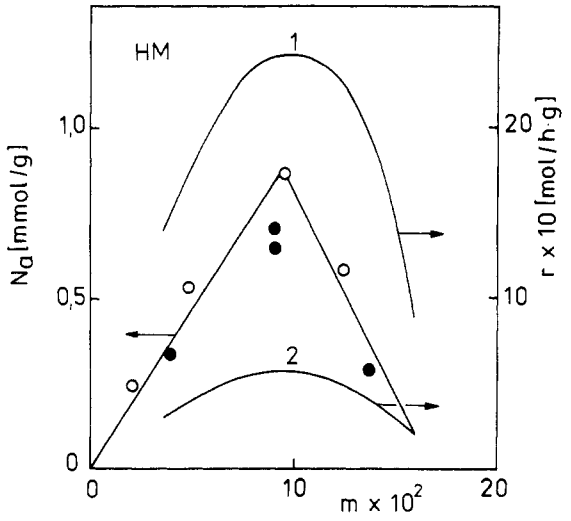


Figure 8. Comparison of catalytic parameters with the number of strong acid site dependence on the mole fraction of tetrahedrally coordinated Al atoms (curve 1, rate of isomerization; curve 2, rate of disproportionation in conversion of *o*-xylene, from ref 43; O, own calorimetric data; ●, calorimetric data from ref 9).

cracking, skeletal isomerization of hydrocarbons, and transformations of alkylaromatics (reviews in refs 12, 36, and 37). This is mainly due to the uniquely high acid strength of the mordenites resulting in a higher rate of hydrocarbon reactions compared with other zeolites. Further important properties are the high chemical and thermal stability and the shape-selective behavior toward large molecules.

All the above-mentioned reactions involve the generation of carbenium ions, including the participation of Brønsted sites. Correlations between the catalytic activity and the acid strength were therefore expected and indeed found. In many cases these correlations are reported in an indirect way, i.e., not between the catalytic activity and the acid strength, but the dealumination degree or the Si/Al ratio, due to the fact that investigations of the acidity were not always performed.

In ref 12 studies of the influence of the dealumination on the mordenite catalytic activity in the cracking of *n*-octane are presented. The activity increases with rising degree of dealumination, passes through a maximum at Si/Al ratio of about 10, and then decreases upon further dealumination. The authors qualitatively explain the activity curve by the increase of the acid strength and the simultaneous decrease of the acid site concentration upon further dealumination. As has been shown, we found a maximum in the concentration of the strong acid sites at a Si/Al ratio of 9.5 (see Figure 6), thus being in a very good agreement with the catalyst possessing a maximum catalytic activity. Maxima in the curves of catalytic activity for dealuminated mordenites with the Si/Al ratio between 8.5 and 10 are also reported for the liquid-phase hydrolysis of ethyl acetate[38] and the isomerization of C_5–C_6 paraffins.[39]

Direct relations between the catalytic activity of alkylaromatics and the number and strength of acid sites in aluminum deficient mordenites were found by Gokhman et al.[40] (toluene disproportionation correlated with the total number of OH groups), Giordano et al.[41] (conversion of *m*-xylene), and Karge et al.[42] (linear relationship between the rate of ethylbenzene disproportionation and the density of Brønsted sites).

Very interesting results were presented by Minachev et al.[43] They investigated the *o*-xylene conversion over dealuminated mordenites with a broad range of Si/Al ratios. The rate of isomerization (curve 1) and disproportionation (curve 2) are plotted against the aluminum molar fraction in Figure 8. The concentration of the very strong acid sites derived from our own measurements and from the literature is included. As may be seen, both curves follow the course of the very strong acid sites, and the maximum in the curves of the catalytic activity corresponds to the maximum of the strong Brønsted acidity.

Conclusions

To investigate the acidity of the samples, four different methods were used: adsorption calorimetry of ammonia, ammonia TPD, ammonium ion exchange, and ^{1}H MAS NMR. The first three methods give values for the total number of Brønsted sites in good agreement, while the mean error of the ^{1}H MAS NMR measurements amounts to about 20%. It was found that the total number of bridged hydroxyl groups rises linearly with increasing number of aluminum atoms in the lattice and that the number of chemisorbed (or exchanged) ammonia molecules per unit cell corresponds to the number of Al_f atoms.

In contrast, the curve of the number of strong acid sites (derived from calorimetric measurements) as a function of aluminum content of the framework passes through a maximum at Al_f = 4.6 (Si/Al = 9.5). By considering the aluminum topological density of different zeolites Barthomeuf predicted a limiting value of Si/Al = 9.4 for the maximum number of strong acid sites in mordenites, this being in excellent agreement with our experimental data. This obviously confirms her theoretical concept.

Comparing the dependence of the catalytic activity of aluminum-deficient H-mordenites in the conversion of hydrocarbons on the Si/Al ratio, maximum values of the activity are found in the region of Si/Al = 8.5–10, this being in good agreement with the composition of the H-mordenite sample investigated with the maximum number of strong acidic sites.

Acknowledgment. The preparation of the mordenite samples by Dr. K. J. Waghamare, NCL Pune (India), is gratefully acknowledged.

Registry No. Al, 7429-90-5; NH_3, 7664-41-7; NH_4^+, 14798-03-9.

References and Notes

(1) Wendt, R.; Jänchen, J., unpublished results.
(2) Tsutsumi, K.; Nishimiya, K. *Thermochim. Acta* **1989**, *43*, 299.
(3) Sawa, M.; Niwa, M.; Murakami, Y. *Zeolites* **1990**, *10*, 532.
(4) Karge, H. G.; Dondur, V. *J. Phys. Chem.* **1990**, *94*, 765.
(5) Meyers, B. L.; Fleisch, T. H.; Ray, G. Y.; Miller, J. T.; Hall, J. B. *J. Catal.* **1988**, *110*, 82.
(6) Chandawar, K. H.; Kulkarni, S. B.; Ratnasamy, P. *Appl. Catal.* **1982**, *4*, 295.
(7) Öhlmann, G.; Jerschkewitz, H.-G.; Lischke, G.; Parlitz, B.; Richter, M.; Eckelt, R. *Z. Chem.* **1988**, *28*, 161.
(8) Klyachko, A. L.; Brueva, T. R.; Kapustin, G. I.; Rubinstein, A. M. *Acta Phys. Chem.* **1978**, *24*, 183.
(9) Klyachko, A. L.; Kapustin, G. I.; Brueva, T. R.; Rubinstein, A. M. *Zeolites* **1987**, *7*, 119.
(10) Auroux, A.; Bolis, V.; Wierzchowski, P.; Gravelle, P. C.; Vedrine, J. C. *J. Chem. Soc., Faraday Trans.* **1979**, *75*, 2544.
(11) Senderov, E. E.; Bychkov, A. M.; Mishin, J. V.; Klyachko, A. L.; Beyer, H. K. In *Zeolites: Facts, Figures, Future*; Jacobs, P. A., van Santen, R. A., Eds.; Elsevier: Amsterdam, 1989; p 355.
(12) Mishin, J. V.; Bremer, H.; Wendlandt, K.-P. In *Catalysis on Zeolites*; Kallo, D., Minachev, Ch. M., Eds.; Budapest, 1988; p 231.
(13) Lohse, U.; Parlitz, B.; Patzelova, V. *J. Phys. Chem.* **1989**, *93*, 3677.
(14) Sohn, J. R.; DeCanio, St. J.; Fritz, P. O.; Lunsford, J. H. *J. Phys. Chem.* **1986**, *90*, 4847.
(15) Lombardo, E. A.; Gaffney, T. R.; Hall, W. K. In *Proc. 9th Int. Congr. Catal.*; Phillips, M. J., Ternan, M., Eds.; Calgary, 1988; Vol. I, p 412.
(16) Topchieva, K. W.; Xo Shu Thoang *Activity and Physico Chemical Properties of High Silica Zeolites and Zeolite Containing Catalysts*; University of Moscow: Moscow, 1976; p 100, and references therein.
(17) Minachev, Ch. M.; Isakov, J. I.; Achmetov, J. S. *Isv. Akad. Nauk SSSR Ser. Chim.* **1976**, *108* and references therein.
(18) Pine, L. A.; Maher, P. J.; Wachter, W. A. *J. Catal.* **1984**, *85*, 476.
(19) Naccache, C.; Cheng Fan Ren; Couduvrier, G. In *Zeolites: Facts, Figures, Future*; Jacobs, P. A., van Santen, R. A., Eds.; Elsevier: Amsterdam, 1989; p 661.
(20) Stach, H.; Jänchen, J.; Lohse, U. *Catal. Lett.* **1992**, *13*, 389.
(21) Freude, D.; Fröhlich, T.; Hunger, M.; Pfeifer, H.; Scheler, G. *Chem. Phys. Lett.* **1983**, *98*, 263.
(22) Wachter, E. A. In *Proc. 6th Conf. Zeolites*; Olson, D., Bisio, A., Eds.; Butterworth: London, 1984; p 141.
(23) Melchior, M. T.; Vaughan, D. E.; Jacobson, A. J. *J. Am. Chem. Soc.* **1982**, *104*, 4859.
(24) Thomas, J. M. In *Proceedings of the 8th International Congress on Catalysis*; Verlag Chemie: Frankfurt, 1984; Vol. 1, p 31.
(25) Mortier, W. J. *J. Catal.* **1978**, *55*, 138.
(26) Kassab, E.; Seiti, K.; Allavena, M. *J. Phys. Chem.* **1988**, *92*, 6705.
(27) Sauer, J. In *Modelling of Structure and Reactivity in Zeolites*; Catlow, C. R. A., Vetrival, R., Eds.; Academic Press, to be published.
(28) Barthomeuf, D. *Mater. Chem. Phys.* **1987**, *17*, 49.
(29) Barthomeuf, D.; Beaumont, J. *J. Catal.* **1973**, *30*, 288.

(30) Dwyer, J.; O'Malley, P. J. In *Keynotes in Energy-Related Catalysis*; Kaliaguine, S., Ed.; Studies in Surface Sciences and Catalysis; Elsevier: Amsterdam, 1988; Vol. 35, p 5.
(31) Dempsey, E. *J. Catal.* **1975**, *39*, 155 and references therein.
(32) Mikovski, R. J.; Marshall, J. F. *J. Catal.* **1976**, *44*, 1700.
(33) Peters, A. W. *ACS Symp. Ser.* **1984**, *248*, 201 and references therein.
(34) Baegley, B.; Dwyer, J.; Fitch, F. R.; Mann, R.; Walters, J. *J. Phys. Chem.* **1984**, *88*, 1744.
(35) Meier, W. M. *J. Solid State Chem.* **1979**, *27*, 149.
(36) Poutsma, M. L. In *Zeolite Chemistry and Catalysis*; Rabo, J. A., Ed.; ACS Monograph; American Chemical Society: Washington, D.C., 1976; p 437.
(37) Barbidge, B. W.; Keen, J. M.; Eyles, M. K. *Adv. Chem. Ser.* **1971**, *102*, 400.
(38) Namba, S.; Hosonuma, N.; Yashima, T. J. *J. Catal.* **1981**, *72*, 16.
(39) Koradia, P. B.; Kiovsky, J. R.; Asim, M. Y. *J. Catal.* **1980**, *66*, 92.
(40) Gokhman, B. Kh.; Gorodetskaya, I. V.; Kaganova, E. M.; Korchagina, I. A.; Tisovsky, G. I. In *Proc. 1st All-Union Conference on the Application of Zeolites in Catalysis*; Novosibirsk, 1976; p 143.
(41) Giordano, N.; Bart, C. J.; Vitarelli, P.; Cavallaro, S.; Ottana, R. In *Proc. Vth Int. Symp. Heterogeneous Catal. Varna* **1983**, *1*, 417.
(42) Karge, H. G.; Weitkamp, J. *Chem.-Ing. Technol.* **1986**, *58*, 946.
(43) Minachev, Ch. M.; Shpiro, E. S.; Mishin, J. V.; Mathe, T.; Antoshin, B. V. *Isv. Akad. Nauk. SSSR Ser. Chim.* **1983**, 2682.

Infrared Study of Ion Beam Deposited Hydrogenated AlN Thin Films. 2. Effect of Deuterium Substitution

Xiao-Dong Wang, K. W. Hipps, and Ursula Mazur*

Department of Chemistry and Materials Science Program, Washington State University, Pullman, Washington 99164-4630 *(Received: January 9, 1992)*

Thin films of amorphous hydrogenated AlN (AlN:H) were prepared by ion beam reactive sputter deposition. Both hydrogenation and deuteration experiments were preformed. Far-IR and mid-IR spectra obtained from these films are presented and vibrational assignments are given. Two new bands are observed at 434 and 501 cm^{-1} in the far-IR region. Al–NH_3 and Al–N_2 are found to be present in hydrogenated AlN films.

Introduction

There is a continuing growth in technological applications of AlN thin films and ceramics. These materials are chemically inert, nontoxic, posses high thermal conductivity, and have excellent piezoelectric and dielectric properties.[1-4] Of special interest is hydrogenated aluminum nitride, AlN:H. The presence of hydrogen improves the electrical and mechanical properties of this material.[5-7] Although there have been several investigations addressing structural properties of stoichiometric AlN[8-10] only a limited number of publications deal with molecular studies of AlN:H.[5,7,11] We have recently reported the mid-IR vibrational spectra and assignments of polycrystalline AlN and amorphous hydrogenated aluminum nitride thin films.[12,13] In this report we present refined assignments for AlN:H based on deuterium isotopic substitution experiments. We also report and assign the far-IR spectrum of the Al–N_2 complex observed in AlN:H films.

Experimental Section

Film Fabrication. Ion beam and thermally deposited films were made in a cryopumped ultrahigh vacuum (UHV) chamber capable of attaining $<10^{-9}$ Torr without baking. The chamber was pumped to $<10^{-7}$ Torr prior to all depositions. Aluminum nitride films 50 nm thick were deposited onto unheated substrates by reactive ion beam sputtering at a rate of 0.02 nm/s. The ion gun was a 2.5-cm low-energy source purchased from Ion Tech, Inc. An FM 4574 gas blender from Linde was used to mix nitrogen and hydrogen gases. The gas mixtures consisted of 100% N_2, 15% H_2:85% N_2, 25% H_2:75% N_2, 35% H_2:65% N_2, 15% D_2:85% N_2, and 25% D_2:75% N_2. Ion beam sputtering was performed at 2×10^{-4} Torr total pressure. The target employed was a 3-in. aluminum disk. A quartz balance was used to measure the deposition rate as well as the thickness of the sputtered films. An Edwards Anavac quadrupole mass spectrometer was used to monitor the atmosphere in the chamber.

Nitride specimens were deposited onto a Au/Al base fabricated on glass substrates. Deposition of the Au/Al film was accomplished through resistive evaporation. An Al film, 200 nm thick, was deposited onto glass from an aluminum-covered tungsten wire. The Al film was then covered with 80 nm of gold. This gold overlayer was evaporated from an aluminum oxide source.

Materials. The substrates used were Corning glass microscope slides. These were cleaned in a solution of 4:1 HNO_3/H_2O_2 prior to use. Concentrated HNO_3 and 30% H_2O_2 were used. Metals of 99.99+% purity were used for all our deposition experiments. All gases used were ultrapure grade. Deuterium gas was purchased from Matheson and was 99% isotopically pure.

FT-IR. Reflectance spectra of AlN films were obtained with an IR/98 FT-IR spectrometer using 83° grazing incidence radiation. The incident light was not polarized. The mid-IR spectra were acquired with 8-cm^{-1} resolution and are the result of 1024 scans. The far-IR data were produced by adding 6048 scans, each of which was collected with 4-cm^{-1} resolution. A helicoil source, and either a germanium-coated KBr (mid-IR) or a 6-μm Mylar (far-IR) beam splitter were employed. A nitrogen-cooled MCT detector and a helium-cooled bolometer (Si/SiGe system from Infrared Associates) were used for the mid- and far-IR data acquisition, respectively. All spectra were obtained at room temperature.

A diffuse reflectance spectrum was obtained from high-purity (99.9%) AlN mixed with KBr (1:5). A KBr:TGS detector and germanium-coated KBr beam splitter were employed. Data were taken at 4-cm^{-1} resolution. The Kubelka–Munk transformation was performed on the reflectance data.

Because there is a large contribution to the far-IR region by the tail on the Al–N mode, we used background subtraction on all the far-IR data. In essence a low order polynomial was fit to the data and then subtracted from it.

Results and Discussion

The upper curve in Figure 1 depicts the vibrational spectrum in the 200–4000-cm^{-1} region of the nitride film made with 15% H_2 in the sputtering gas mixture. The bottom trace displays the far- and mid-IR reflectance spectra obtained from an AlN film fabricated with 15% D_2 and 85% nitrogen. The far-IR portions of the spectra have been scaled by a factor of 20. The positions of the vibrational bands present in these spectra are collected in

0022-3654/92/2096-8485$03.00/0 © 1992 American Chemical Society